

# Particle acceleration in ultra-relativistic parallel shock waves

A. Meli<sup>a,b,1</sup> and J.J. Quenby<sup>a</sup>

<sup>a</sup>*Astrophysics Group, Blackett Laboratory, Imperial College of Science, Technology and Medicine, Prince Consort Rd. SW7 2BW, London, UK.*

<sup>b</sup>*Visiting Max Planck Institut fuer Radioastronomie, Auf dem Huegel 69 53121, Bonn, Germany.*

---

## Abstract

Monte-Carlo computations for highly relativistic parallel shock particle acceleration are presented for upstream flow gamma factors,  $\Gamma = (1 - V_1^2/c^2)^{-0.5}$  with values between 5 and  $10^3$ . The results show that the spectral shape at the shock depends on whether or not the particle scattering is small angle with  $\delta\theta < \Gamma^{-1}$  or large angle, which is possible if  $\lambda > 2r_g\Gamma^2$  where  $\lambda$  is the scattering mean free path along the field line and  $r_g$  the gyroradius, these quantities being measured in the plasma flow frame. The large angle scattering case exhibits distinctive structure superimposed on the basic power-law spectrum, largely absent in the pitch angle case. Also, both cases yield an acceleration rate faster than estimated by the conventional, non-relativistic expression,  $t_{acc} = [c/(V_1 - V_2)][\lambda_1/V_1 + \lambda_2/V_2]$  where '1' and '2' refer to upstream and downstream and  $\lambda$  is the mean free path. A  $\Gamma^2$  energy enhancement factor in the first shock crossing cycle and a significant energy multiplication in the subsequent shock cycles are also observed. The results may be important for our understanding of the production of very high energy cosmic rays and the high energy neutrino and gamma-ray output from Gamma Ray Bursts (GRB) and Active Galactic Nuclei (AGN).

---

## 1 Introduction

There are three distinct astrophysical situations where the bulk plasma flow is extremely relativistic with Lorentz factors  $\Gamma = (1 - V^2/c^2)^{-1/2} \geq 10$ . These are some Active Galactic Nuclei (AGN) jet and hot spot sites, Gamma Ray

---

<sup>1</sup> Corresponding author: a.meli@ic.ac.uk

Burst (GRB) fireballs and pulsar polar winds. Within these flows relativistic shocks appear and diffusive particle acceleration takes place. In each case, there is evidence for energetic particle acceleration to high  $\Gamma$  factors but the upper limit to the possible energy attained becomes less certain with increasing bulk flow velocity. For AGN jets,  $\Gamma \sim 10$  plausibly results in the known  $10^{19}$  eV cosmic rays (Quenby and Lieu, 1989) via diffusive shock acceleration at the termination shocks. However, the more direct synchrotron/self-Compton modeling only reveals 10 GeV gamma-rays (e.g. Maraschi et al., 1992). For GRB fireballs,  $\Gamma \sim 100 - 10^3$  appears to eventually produce gamma-rays at least up to 100 MeV (Fenimore et al., 1993) but at such flow speeds, it is not clear whether repeated shock crossings are possible and the predictions of  $10^{19}$  eV neutrinos (Vietri, 1998), which would be direct evidence of a diffusive like process have yet to be verified. Similarly, pulsar winds could result in a  $\Gamma \sim 10^4$  flow encountering the nebula envelope (Hoshino et al., 1992), but there is no evidence for more than TeV acceleration anywhere in the system. However Lucek and Bell (1994) show that combined motion across a near perpendicular shock with a non-uniform field and in the electromagnetic field of the nebula may produce much higher energies.

Past work has suggested that if the shocks are close to parallel so that an  $\mathbf{E} = 0$  frame can be defined, diffusive shock acceleration is in principle possible and provided large angle scattering occurs in the plasma frame, each shock crossing cycle yields a  $\sim \Gamma^2$  energy increase (Quenby and Lieu, 1989). This result has been exploited by Vietri (1995,1998) modeling GRB fireball particle shock acceleration. It is the purpose of this paper to present simulation results on particle acceleration with  $\Gamma$  values extended up to  $\sim 10^3$ . Here we concentrate on the parallel shock configurations ( $\psi = 0^\circ$ ). Our results, measured in the shock frame, will be compared with the standard spectral prediction of non-relativistic theory, where the momentum spectrum is  $n(p) \propto p^{-\alpha}$  with  $\alpha = (r+2)/(r-1)$ , for shock compression ratio  $r = V_1/V_2$ , independent of scattering details, and  $\alpha = 2$  for strong unmodified shocks with  $r = 4$ . Analytically it has been shown that over a limited momentum range, the non-relativistic time scale for acceleration is  $T = [c/(V_1 - V_2)][\lambda_1/V_1 + \lambda_2/V_2]$  where, '1' and '2' refer to upstream and downstream and  $\lambda$  is the scattering mean free path. The shock jump solutions of Ballard and Heavens (1991) and the review of Kirk and Duffy (1999) show that, a range of shock frame  $r$  values largely limited between 3 and 4, typically arise for oblique, relativistic shocks, whereas  $r=4$  is the extreme relativistic hydrodynamic limit. Hence for simplicity we adopt  $r=4$  but, in the companion paper dealing with oblique shocks we demonstrate the insensitivity of our chief conclusions on the exact value. For our parameters,  $T = (8/3)(nr_{g,1}/c)$  where,  $\lambda = nr_g$  and  $r_g$  is Larmor radius.

The first relativistic correction noticed to the non-relativistic theory, was the spectral flattening seen in parallel shocks (Kirk and Schneider, 1987a,b), followed by the discovery of a speed-up in the acceleration rate (Quenby and Lieu, 1989; Ellison et al., 1990). These results have subsequently been extended to non-parallel and non-linear sub-luminal shocks (Lieu, et al., 1994

and Bednarz and Ostrowski, 1996 who use  $T = r_g/c$  as the unit of acceleration time), where there is large angle scattering or pitch angle diffusion. Most recently, much interest has been focused on differences occurring between small angle and large angle scattering models for the test particle-turbulence interactions in the fluid frame. Gallant and Achterberg (1999) suggest that for a field model consisting either of randomly orientated uniform field cells or a uniform field, the scattering is limited to  $\delta\theta < 1/\Gamma$  in the upstream fluid frame. Generally, such a model yields a test particle differential spectral slope  $\sim -2.2$  (Baring, 1999). Furthermore, on this model, Gallant and Achterberg (1999) provided an analytical demonstration that in the high  $\Gamma$  limit, only the first crossing cycle exhibited a  $\Gamma^2$  energy increase, while in all other crossings the energy is only doubled and hence one may expect the relativistic speed-up to be limited to this crossing. The computations of Baring (1999) also showed a much reduced energy enhancement in subsequent cycles for the small angle scattering case. Achterberg et al. (2001) extend the conclusions of Gallant and Achterberg (1999) to a wider variety of upstream field models while, Kirk et al. (2000) employ an eigenfunction method to deal with the anisotropies in diffusion when the scattering depends on the angle with the shock normal. A recent general review of particle acceleration and relativistic shocks is given by Kirk and Duffy (1999). However, the detailed contrast between the effects of various particle scattering models and the behaviour of these models at  $\Gamma$  factors  $\sim 10^3$  remain to be elucidated, both for parallel and quasi-perpendicular shocks. Hence this paper starts a series of investigations in the ultra-relativistic limit with a consideration of parallel shocks. In section 2 we present the numerical method used, section 3 presents the results while in section 4 conclusions and consequences are given. A further paper seeks to extend this work to non-parallel shocks (Meli and Quenby, 2002b).

## 2 Numerical Method

The actual purpose of these simulations is to find a solution to the particle transport equation for highly relativistic parallel flow velocities. The appropriate time independent Boltzmann equation is given by the following as we assume steady state,

$$\Gamma(V + v\mu)\frac{\partial f}{\partial x} = \frac{\partial f}{\partial t}|_c \quad (1)$$

where  $\Gamma$  is the Lorentz factor of the fluid frame,  $V$  is the fluid velocity,  $v$  the velocity of the particle,  $\mu$  the cosine of the particle's pitch angle and  $\frac{\partial f}{\partial t}|_c$  the collision operator. The reference frames we use during the simulations are the upstream and downstream fluid frames and the shock frame. Pitch angle is measured in the local fluid frame, while  $x$  is in the shock rest frame

and the model assumes variability in only one spatial dimension. In order for the above equation to be solved by a simple Monte Carlo technique, we assume that the collisions represent scattering in pitch angle with no cross-field diffusion, the scattering is elastic in the fluid frame and a phase averaged distribution function may be employed. We will discuss these assumptions in more detail in due course. The collision operator may be characterized by two types of scattering that the particles suffer, large angle and small angle scattering, which are respectively represented by the two following equations:

$$\frac{\partial f}{\partial t}|_c = \frac{\langle f \rangle_\mu - f}{\tau} \quad (2)$$

where  $\tau$  is the mean time between collisions, related to the mean free path by the relation  $\lambda = v\tau$  and,

$$\frac{\partial f}{\partial t}|_c = \frac{\partial}{\partial \mu} \left( D_{\mu\mu} \frac{\partial f}{\partial \mu} \right) \quad (3)$$

where  $D_{\mu\mu}$  is the pitch angle diffusion coefficient. As mentioned previously, Gallant and Achterberg (1999) have demonstrated that small angle scattering with  $\delta\theta < 1/\Gamma$  applies with  $\theta$  measured in the upstream fluid frame for scattering in a uniform field or a randomly orientated set of uniform field cells. This arises because particles attempting to penetrate upstream from the shock are swept back into the shock before they can move far in pitch. To establish the conditions for large angle scattering, we demand the particle penetrating upstream can move over about a Larmor radius,  $\sim r_g$ , on encountering the scattering centre while still upstream. A suitable scattering centre would be a rotational discontinuity or a much enhanced field region. Let  $v$  be the particle velocity in the shock frame, directed perpendicular to the shock in the upstream direction, the most favourable case for re-entry upstream. If  $v \sim c$ , transforming to the upstream frame via  $v_1 = (v - V_1)/(1 - \frac{vV_1}{c^2})$  and allowing  $V_1 = c - \delta \sim c$  yields  $v \sim c$ . Now in the upstream frame, the shock velocity is  $-c + \delta$ , if the positive spatial coordinate,  $x$ , is towards the shock. If  $\lambda_1$  is the mean free path for scattering (encountering a large angle scatterer) in the upstream frame, the average time to reach this scatter centre after leaving the shock is  $\Delta t_1 = \lambda_1/c$ . Meanwhile, the shock moves in the upstream frame a distance  $(c - \delta)\Delta t_1$ . Hence we require  $r_{g,1} < \lambda_1 - (c - \delta)\Delta t_1$  to allow space for the upstream large angle scatter to occur. If  $\Gamma_1 = [1 - (V_1^2/c^2)]^{-0.5}$ , we find  $r_g < \lambda_1/2\Gamma_1^2$  as the condition for large angle scattering.

The most favourable site to find high  $\Gamma$  large angle scattering is in GRB which may arise from collapse resulting in a rapidly rotating black-hole torus system (van Putten, 2001). Rotation allows a  $1/r$  field and we start from a torus of about one Schwarzschild radius, depending on spin, of a  $20M/M_\odot$  hypernova collapse and the presence of a field near the torus of about  $B_\odot = 10^{14}$  gauss. Although Brainerd (1992) shows that for typical GRB parameters and a cos-

mological jet model, cyclotron and synchrotron radiation are only possible for fields below about  $10^{10}$  gauss, his arguments apply only to the regions from which emission emerges. Lieu et al. (1989) are among authors pointing out the extra quantum mechanical processes arising at  $\Gamma B > 10^{14}$ , thus suggesting that the maximum possible field strength, which could arise in equipartition with the burst binding energy,  $\sim 10^{18}$  gauss, will rapidly reduce in strength as discussed by Lerche and Schramm (1977). Blobs, rather than a steady 'wind' arise in some models (e.g. Blackman et al., 1996). Meszaros et al. (1993) suggest a comoving fireball size during the main acceleration phase  $r_{b,1} \sim 10^{14} \rightarrow 10^{16}$  cm and a mean fireball field just due to equipartition with internal shocks of  $B_{a,1} \sim 10^2$  gauss. The suffix '1' is used for comoving quantities and this suffix is omitted for fixed frame quantities. The transverse comoving frame 'bullet' fields which are likely to be effective for our scattering are estimated by  $B_s = B_o r_o / r$  where  $B_1 = B / \Gamma$  and  $r_1 = \Gamma r$ . Let  $\lambda_{a,1}$  be the parallel mean free path in the ambient or general shocked field outside the 'bullets' with,  $\lambda_{a,1} = n r_{g,a,1}$  where,  $r_{g,a,1}$  is Larmor radius and  $n > 10$  as suggested by detailed computations in the turbulent interplanetary medium (Moussas et al., 1992 and references therein). Diffusive shock acceleration can hardly be expected unless the mean free path is significantly smaller than the dimensions of the region. Also  $r_g \propto \gamma$ , the particle Lorentz factor. Hence we may write  $\lambda_{a,1} = \min[r_{b,1}/10, n \rho_{1,a}]$ . Then inserting this expression in our large angle scatter limit requires either  $B_{a,1}/B_{s,1} < n/2\Gamma^2$  independent of  $\gamma$  or,

$$p_1(\text{eV}) < \frac{300 B_{s,b,1} r_{b,1}}{10 \times 2\Gamma^2} (\text{gauss}, \text{cm}) \quad (4)$$

where, the particle momentum  $p_1$  and field  $B_{s,b,1}$  are measured near the fireball boundary. Taking the extreme  $\Gamma = 10^3$ , with  $n = 40$ , the first inequality is marginally satisfied if  $r_{b,1} \leq 10^{14}$  cm while the second inequality is satisfied at a moving frame momentum of  $< 10^{16}$  eV or rest frame momentum of  $< 10^{19}$  eV. Thus, it is possible to envisage GRB models with  $\Gamma < 10^3$  where large angle scattering is occurring, especially if a larger torus or torus field is allowed.

Here we consider one-dimensional parallel shocks ( $\psi = 0^\circ$ , where  $\psi$  is the angle between the shock normal and the magnetic field), either because that is the field configuration, or because turbulence removes 'reflection' at the interface even though the magnetic field does not lie along the  $x$ -axis. A test particle approximation is used for simplicity to allow a step by step approach to understanding the full problem, though eventually non-linear effects must be included. Relativistic particles of initial  $\gamma \sim (\Gamma + 10)$  are injected upstream towards the shock and are allowed to scatter in the respective fluid frames with their basic motion described by the guiding centre approximation. One justification is we note that Bell (1987) and Jones and Ellison (1991) have shown that 'thin' sub-shocks appear even in the non-linear regime, so at some

energy above the plasma value, the accelerated particles may be dynamically unimportant while they recross the discontinuity. Another way of arriving at the test particle regime is if particles are injected well above the plasma particle energy, remaining dynamically unimportant and thus requiring the seed particles to have been already pre-accelerated. In AGN jets, traveling shocks superimposed on the relativistic flows accelerated by pressure at the jet base, could provide the seed for the terminal 'hot spot' acceleration. Such seed particles appear in the neutron star binary merger scenario for GRB (Narayan et al., 1992), which includes the presence of pre-accelerated particles before any terminal shock acceleration phase, possibly due to explosive reconnection. For isolated pulsars, we note that there is strong observational evidence (e.g. PSR1913+16, PSR2127+11C) for the continuous injection of relativistic particles into the surrounding medium, over their lifetime. While this plasma will probably be predominantly in the form of  $e^+e^-$  pairs, created in the pulsar magnetosphere, it has been argued that pulsar winds must also contain ions in order to account for the electric currents in the Crab Nebula (Hoshino et al., 1992; Gallant and Arons, 1994). These authors employ a wave acceleration process at the shocked termination of the flow, to provide a non-thermal pair spectrum to yield the X-ray and gamma-ray output. However their input distribution function is also not mono-energetic and therefore containing 'seed particles' above the bulk flow energy. The supposed nature of the slot/gap electric field acceleration of the pair plasma is unlikely to give a mono-energetic output.

A relativistic transformation is performed from the local plasma frames to the shock frame to check for shock crossings. In this parallel shock case, there is no reflection allowed and on crossing the computation is continued in the other plasma frame. We change units so that  $m \approx c = 1$ . The particle is made to leave the system if it 'escapes' far downstream at the spatial boundary, or if it reaches a well defined maximum energy  $E_{max} = E_o 10^{14}$ , for computational convenience, even though other physics describing particle escape or energy loss would probably need to be taken into account in realistic situations. The downstream spatial boundary required can be estimated from the solution of the convection-diffusion equation in a non-relativistic, large-angle scattering approximation in the downstream plasma which gives the chance of return to the shock,  $exp(-V_2 r_b / D)$ , yielding a probability of return of  $2 \cdot 10^{-3}$  if  $r_b = 8 \lambda_{||}$ . In fact, runs are performed with different spatial boundaries to investigate the effect of the size of the acceleration region on the spectrum, as well as to find a region where the spectrum is size independent. In the small-angle scatter case, the inherent anisotropy due to the high downstream sweeping effect may greatly modify this analytical estimate.

The particles ( $\sim 10^5$ ) of a weight ( $w_p$ ) equal to 1.0, are injected far upstream and they are allowed to move towards the shock, along the way colliding with the scattering centers. Provided multiple scattering between the upstream and downstream regions of the shock can occur and they gain energy in each crossing, diffusive shock acceleration is simulated. The compression ratio ( $r$ ) is kept

at the value of 4 for simplicity.

A splitting technique is applied, similar to Bednarz and Ostrowski's (1998) in order to obtain statistical accuracy over a wide range of particle Lorentz factors. The splitting technique helps to avoid the consequence that in highly relativistic flow environments, only a few high energy accelerated particles, which remain in the acceleration process, dominate the recorded distribution function, thereby limiting the statistical accuracy to an energy range of only two or three decades above injection energy  $E_o$ . By introducing more particles, but of corresponding lower weight when some energy well above injection is attained, a greater sampling of the possible regions within the accessible phase space of the model is achieved.

The mean free path  $\lambda$  for particle scattering is calculated in the respective fluid frames and if it is assumed that it is dependent on the particle's energy as given by the formula,  $\lambda = \lambda_o p \cos\theta$ , where  $\theta$  is the particle's pitch angle, so as to allow for a particle 'current' and phase space weighting, the probability that a particle will move a distance  $x$  along the field lines at pitch angle  $\theta$  before a scattering is given by the expression,  $p(x) \propto \exp(-x/\lambda)$ . At the scattering centers the energy (momentum) of the particle is kept constant and only the direction of the velocity vector  $v$  is randomized, using a computational random number generator. The downstream mean free path is taken as a factor 4 less than upstream while the absolute value is arbitrary since the model boundaries are specified in units of the mean free path.

To model the large angle scatter case, the new pitch angle is chosen at random (phase angle is neglected in this guiding centre approximation but will need to be chosen to specify the scattering). For the picture of pitch angle diffusion case, we assume that the tip of a particle's momentum vector undergoes randomly a small change  $\delta\theta$  in its direction on the surface of a sphere and within a small range of polar angle (after a small increment of time) (Ellison et al., 1990). If the particle had an initial pitch angle  $\theta$ , we calculate its new pitch angle  $\theta'$  by the simple trigonometric formula,

$$\cos\theta' = \cos\theta\sqrt{1 - \sin^2\delta\theta} + \sin\delta\theta\sqrt{1 - \cos^2\theta\cos\phi} \quad (5)$$

where,  $\phi \in (0, 2\pi)$  is the azimuth angle with respect to the original momentum direction and must be chosen at random in this case. For the case of highly relativistic flows, we limit particles pitch angle diffusion to angles chosen at random, up to an angle  $\sim 1/\Gamma$ , where  $\Gamma$  is the upstream gamma, measured in the shock frame (Gallant and Achterberg, 1999) in order to be consistent with these authors' model for upstream re-entry but some runs are performed with the scattering angle  $\sim 0.1/\Gamma$  to correspond to the later work of Achterberg et al. (2001) and Protheroe et al. (2002) -private communication.

A consequence of this limitation in upstream scatter for the Gallant and Achterberg (1999) model follows if we calculate the ratio of energies cross-

ing down-upstream measured in the respective fluid frames as  $\Gamma(1 + \beta_r \mu'_{\rightarrow u})$  where  $\beta_r$  is the relative velocity of the two streams as a fraction of  $c$  and  $\mu_{\rightarrow u}$  is cosine pitch angle for down to upstream crossing in the downstream frame. This angle only needs to exceed  $1/4 \rightarrow 1/3$  for kinematic reasons. Hence the energy gain can still be  $\sim \Gamma$  in contrast to the gain ratio for the up to down transition which is  $\Gamma(1 - \beta_r \mu_{\rightarrow d})$  and where,  $\mu_{\rightarrow d}$  the upstream frame cosine pitch angle on up to down transmission is nearly unity due to the limitation on the scattering permissible.

This prediction of limited energy gain on all crossings subsequent to the first cycle, will be investigated in our simulations, as it is important to establish the dependence of the model results on whether or not large angle or pitch angle diffusion operate in highly relativistic flows.

### 3 Results

First, test runs to verify the validity of the codes which have been performed in the mildly relativistic limit (e.g.  $V_1 = 0.1c - 0.6c$ ) tend to excellent agreement with the non-relativistic theory, giving smooth spectra shapes and spectral indexes close to -2.2. In addition, similar runs show that as the flow becomes more relativistic, the spectrum flattens, which is in agreement with the analytical and numerical work of Kirk and Schneider (1987a,b). We also compare our results with similar studies for  $\Gamma \sim 5$  (Baring, 1999) and find agreement concerning the spectral index and the spectral shape for both large angle scattering and pitch angle diffusion mechanisms.

As we have already mentioned a compression ratio ( $r$ ) of 4 is used for simplicity and also to allow immediate comparison with non-relativistic unmodified strong shock results, but our preliminary code runs show that the qualitative trend of the results is insensitive to the exact compression ratio value, due to the mildly-relativistic nature of the downstream plasma. Initial Lorentz factors of the flow investigated are 5, 50, 200, 500 and 990.

All results are given at the shock, in the shock frame. The particle distribution function is obtained in a particular energy and  $\mu$  space cell by recording the passage of each simulation particle crossing the cell, weighted by the time taken in cell crossing.

In figure 1 we show the ratio of the computational time constant to the non-relativistic analytical acceleration time constant, as defined in the 'Introduction' section, calculated as a function of the upstream Lorentz factor  $\Gamma$  flow for large and small angle scattering. Note that we are effectively measuring 'speed-up' of the acceleration time in units of a few times  $r_g/c$ .

We obtain the time constant  $t_{acc}$  from the computation by recording the energy increment for each complete cycle, up-down-up and the time taken for the cycle



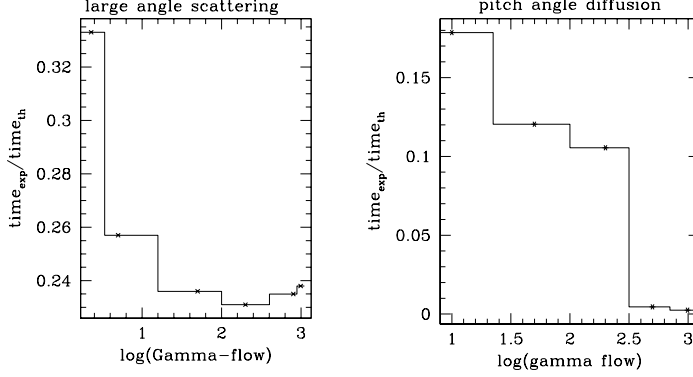


Fig. 1. The ratio of the computational time to the non-relativistic analytical constant (measured in the shock frame) versus the logarithm of the Lorentz  $\Gamma$  flow, for large angle scattering (left) and for pitch angle diffusion (right).

at a particular energy level,  $\Gamma$  and finding the mean increments,  $\Delta\Gamma$  and  $\Delta t$ . Then  $t_{acc}/\Delta t = \Gamma/\Delta\Gamma$ . We find a 'speed-up' of about a factor of 5 for large angle scattering and a considerable speed-up of a factor  $\sim 20$  for pitch angle diffusion. In this latter case, the parallel mean free path is estimated for the analytical formula from the time to multiple scatter in pitch angle through  $\pi/2$ . That is  $\lambda_{\parallel} = (\pi^2/4)(c\lambda/\delta\theta^2)$  where  $\lambda \propto \gamma$  is the step length between collisions yielding  $\delta\theta$ .

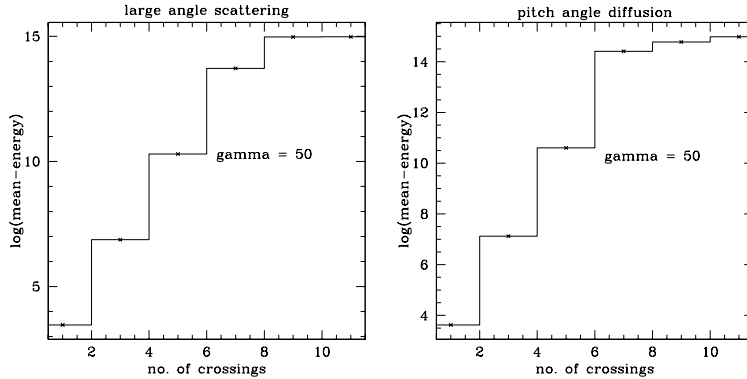


Fig. 2. The logarithm of the mean-energy gain of particles versus the no. of shock crossings (1-3-5-7-9-11), where upstream  $\Gamma$  equals 50. The energy is measured immediately after the particle has crossed the shock front. Large angle scattering (left), pitch angle diffusion (right).

Particle energy is specified in units of  $\gamma$  and hence applies both to electron and ion acceleration. Figures 2 and 3 show the logarithm of the particle's mean-energy against the number of shock crossings for the two scattering models, at  $\Gamma=50$  and 990. Here crossings 1 to 3 (downstream  $\rightarrow$  upstream  $\rightarrow$  downstream) represent one cycle.

The energy is measured immediately after the particle has crossed the shock front in the shock frame. In all cases, the energy gain on the first complete cycle, specified by crossing numbers 1 and 3 is  $\sim \Gamma^2$  but subsequent crossings

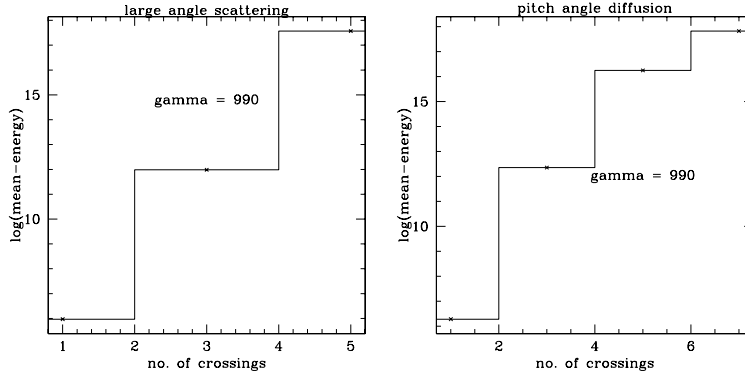


Fig. 3. The logarithm of the mean energy gain of particles versus the no. of shock crossings, employing an upstream flow gamma factor  $\Gamma=990$ . The energy is measured immediately after the particle has crossed the shock front. We observe a  $\Gamma^2$  energy boost in the first to the third crossing and significant energy multiplication in all subsequent crossings. Large angle scattering (left), pitch angle diffusion (right).

show a reduced gain, passing through a region where the increase is ( $\sim \Gamma$ ) and tending towards the factor  $\sim 2$  predicted by Gallant and Achterberg (1999).

However, the gain reduction is slower than expected by these previous authors and the qualitative idea expressed above. The discrepancy could lie in details of the scattering model in that the computation assumes negligible scattering before the first scatter centre is reached, equivalent to almost undeviated guiding centre motion along a field line, whereas the Gallant and Achterberg (1999) approach takes the opposite extreme of continued deflection in a plane at a large angle to a uniform field.

In figure 4 the angular distribution is measured in the shock frame just downstream for the upstream to downstream transition and just upstream for the down to up transition, for large angle scattering and upstream flow  $\Gamma = 200$ . Similar plots for small angle scattering (pitch angle diffusion case) are also presented. We only show the contribution to the distribution function of particles which have just crossed, not the complete time averaged distribution. Similar results were obtained for  $\Gamma = 10 - 990$ . It is evident that there is extreme peaking in the angular distribution towards smaller pitch angles in all but one case, continuing the trend noticed by Quenby and Lieu (1989) and Ellison et al. (1990) at lower flow  $\Gamma$ , who found that as the velocities become more relativistic the anisotropies in pitch angle become greater. If the distribution function at the shock is isotropic, the number of particles between  $\mu$  and  $\mu + \Delta\mu$  is proportional to  $\mu$ , taking into account solid angle weighting.

Both scattering cases reveal highly peaked distributions pointing downstream on up to down transition, due to the beaming of the upstream distribution function as seen by the shock. Downstream to up for large angle scattering produces near triangular distributions in the upstream directed half space, due to the very efficient scattering in the model. For small angle scattering, highly

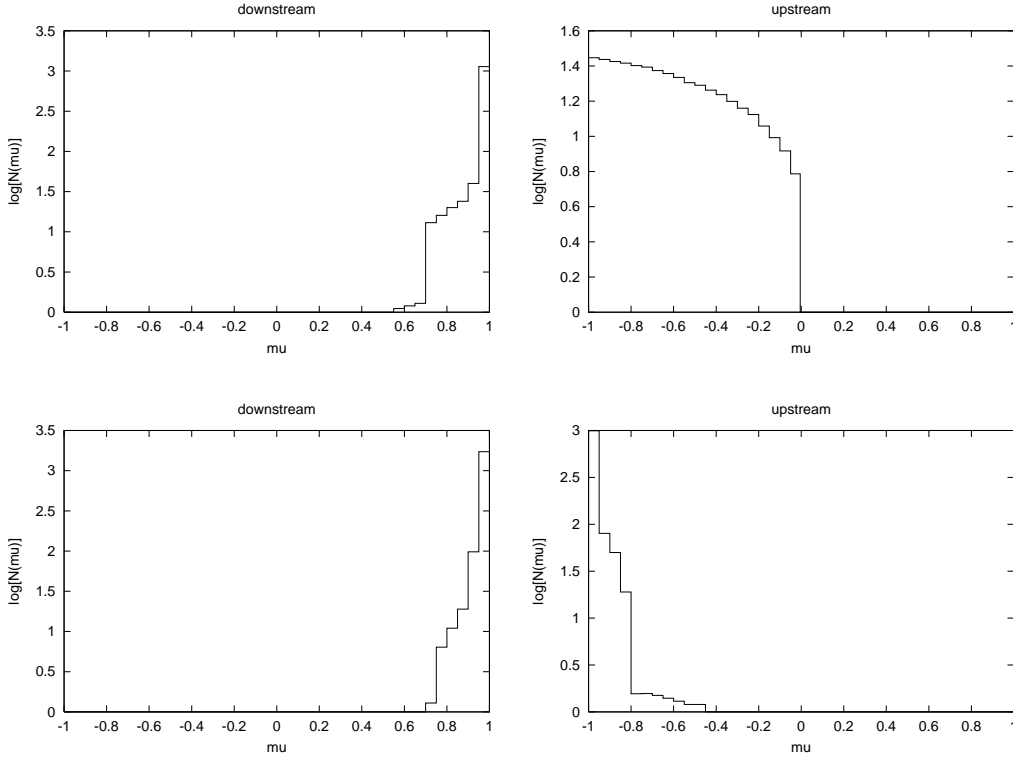


Fig. 4. Angular distribution ( $\mu = \mu = \cos\theta$ ) in the shock frame for  $\Gamma = 200$ , after the particles have crossed the shock from upstream  $\rightarrow$  downstream (left) and downstream  $\rightarrow$  upstream (right). Top plots for large angle scattering, bottom plots for pitch angle diffusion.

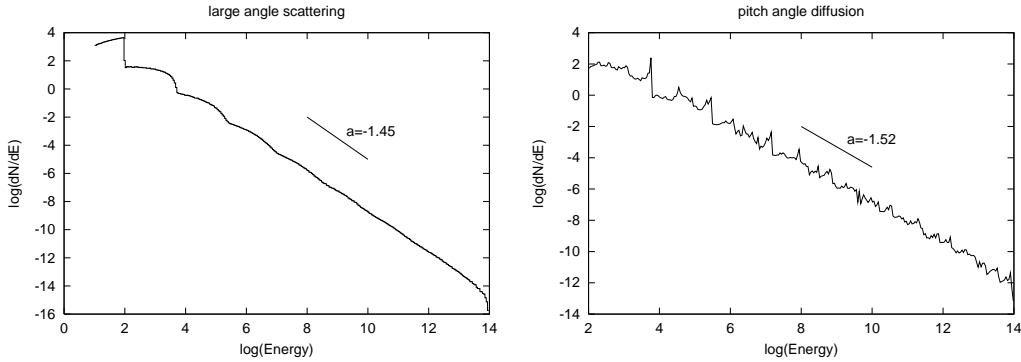


Fig. 5. Spectral shape for upstream  $\Gamma=5$ . Large angle scattering (left) pitch angle diffusion (right). The line shows the mean slope of the spectrum and the number is the spectral index found. The smoothness (compared to higher gamma flows used) and the spectral index (especially for the large angle scattering) are consistent with similar work presented by Baring (1999).

peaked distributions are found due to the lack of time for significant deflection from nearly zero pitch angle before downstream re-entry and presumably for those particles which can re-enter upstream.

In figures 5,6 and 7 we show the spectral shapes obtained at the shock just

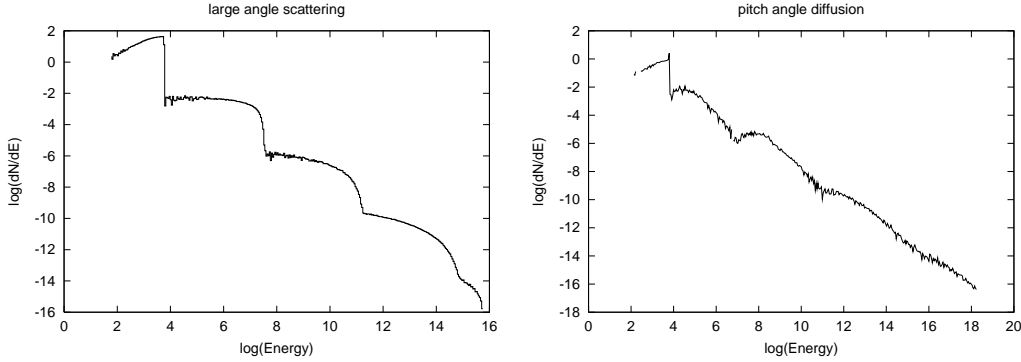


Fig. 6. Left, the spectral shape, for an upstream  $\Gamma=50$ , for large angle scattering. Right, the spectral shape for the same gamma, for pitch angle diffusion.

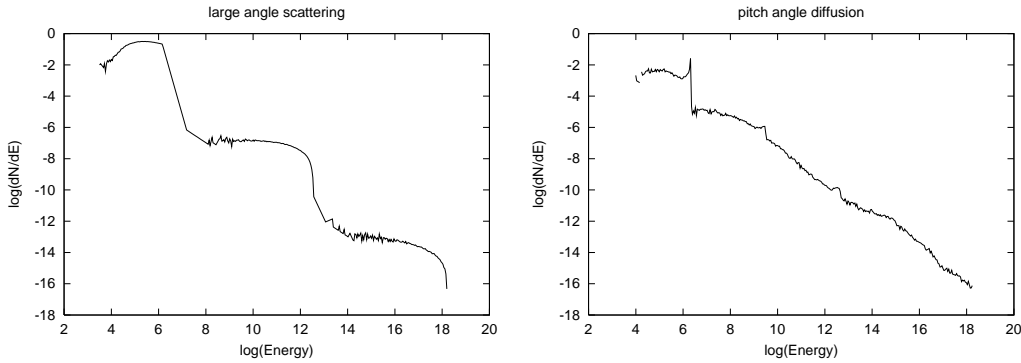


Fig. 7. Left, the spectral shape for an upstream  $\Gamma=990$ , for large angle scattering. Right, the spectral shape for an upstream  $\Gamma=990$ , for pitch angle diffusion.

downstream, for large and small angle scattering (pitch angle diffusion) for upstream flow  $\Gamma$  values of 5, 50 and 990 respectively. We investigated the sensitivity of these spectral shapes for small angle scattering to downstream boundary condition, and found that the shapes did not change significantly for the boundary distance,  $r_b \geq 2 \cdot 10^3 \lambda$ . Probably the small chance of return to the shock except for a relatively small subset of downstream pitch angle particle 'histories', produced this result and the anisotropy in figure 4 is seen for these returning particles. Note the relatively smooth spectra for the relativistic flow with  $\Gamma = 5$  (fig. 5) which becomes plateau-like at the more extreme value of  $\Gamma = 990$  (fig. 7) where the effects of individual acceleration cycles are clearly evident in the large angle case, but not for small angle scattering, where the spectral shape remains rather 'smooth'. Features can be seen developing in the lower  $\Gamma$  simulations of Quenby and Lieu (1989) and Ellison et al. (1990) while Protheroe (2001) shows a similar contrast in behaviour, between large and small angle scattering models up to  $\Gamma = 20$ . On any individual cycle, greater energy gain is available for the large angle case because of the greater upstream scattering, as demonstrated in the simple analytical approach mentioned above.

Hence, the plateaus develop for the large angle case with flatter segments,

than the smoother pitch angle case spectrum. An opposing effect, however, is that because the accelerated particles re-entering downstream have pitch angles more favourable to eventual loss downstream, the drop between plateaus is greater and so the overall spectral slopes in the two cases are rather similar. The actual mean slope of the differential number spectrum is well above -2, as illustrated by the lines of slope -1.45 and -1.52 shown for  $\Gamma=5$ . This relativistic flattening effect is consistent with previous studies by Baring (1999) while, the mechanism of plateau development as an acceleration cycle effect is implicit in figure 6 of Protheroe (2001). It is perhaps not surprising to observe a step-like behaviour in the accelerated spectrum, clearly related to groups of particles undergoing different numbers of acceleration cycles, because the simulations also reveal that about 90% of all particles in the simulation box are lost downstream each cycle. One might also expect that small angle scattering has the greater chance of smoothing the inherent structure in the acceleration process. Clearly, smoothing is much more efficient at lower flow  $\Gamma$  where the gain per cycle is less.

One can infer that at extreme relativistic flow velocities and different scatter models, it is difficult to assume that the spectral shape of the accelerated particles follows a *smooth* power-law shape, as in the classic non-relativistic first order Fermi acceleration mechanism, under all circumstances.

## 4 Conclusions

To what extent is first order Fermi acceleration universally applicable in shocked, turbulent, MHD flows ? Aspects of the problem still needing elucidation include the spectrum produced, the spectral index, the angular distribution of the particles and non-linear effects in relativistic flows.

We have presented a detailed Monte Carlo approach for the highly relativistic diffusive acceleration in parallel shocks under the test particle approximation, extending previous studies to more extreme values of the upstream flow  $\Gamma$  and carefully distinguishing the effects of different assumptions concerning the particle scattering. Comparison is made with results under non-relativistic conditions. It is found that the spectral shape in the very relativistic flow regime depends on the scatter model (large angle or pitch angle diffusion/small angle scattering), with the former model exhibiting a structure in the spectrum at the shock related to the cycle of acceleration, while the later one showing a smoother shape. One general indication which supports the validity of our computational approach is that the spectral index becomes flatter as the flow becomes more relativistic, a result to be compared with the conclusions of Kirk and Schneider (1987a,b).

Extreme anisotropy in the shock frame for particles emerging downstream irrespective of scattering model is observed, due to the beaming of the trans-

mitted flux. High anisotropy also occurs in the flux emerging upstream in the small angle scattering case, due to the lack of time to isotropize the particles but in the large angle scattering model there is a large enough probability of scatter before shock re-entry for near isotropy to set in. This means that for any given acceleration cycle, the spectrum is much flatter in the large angle case (plateaus) because the gain per cycle can be greater. However, evidently because of an enhanced loss downstream of the more scattered particles of the large angle scattering case, the average spectral slope for the two mechanisms is similar.

Most important, a significant acceleration rate increase ('speed up' effect) has been found for both large angle and pitch angle diffusion. This must be seen in conjunction with a 'gamma-squared' energy boosting of the particle noted in the first shock cycle, which is in accordance with theoretical indications (e.g. Gallant and Achterberg, 1999) and past simulations (e.g. Lieu and Quenby, 1989). There is a gain by a significant factor in subsequent crossings which is  $\sim \Gamma$  or even more for several cycles. Regarding the acceleration time decrease, computations show that the comparison of the simulation (experimental) acceleration time with the analytic non-relativistic time constant, indicates a decrease of about 5 with increasing flow gammas ( $10$ - $10^3$ ). This speed-up is clearly directly related to the boosting of the energy gain.

In the theory of GRB production (Meszaros and Rees, 1993) by cosmic fireballs, the  $\Gamma \sim 10^3$  flows are expected to produce some shock acceleration of electrons and protons. Vietri (1995) suggests protons of  $\gamma \leq 10^{11}$  produce photons of 300 GeV by proton synchrotron radiation and neutrinos of  $10^{19}$  eV via photopion production and subsequent cascading. This requires only two shock acceleration cycles at flow  $\Gamma \sim 10^3$ , a suggestion well supported by the results obtained here for both scattering models. However, at these high  $\Gamma$  values, extreme 'billiard ball' scattering is required over distances much less than  $\lambda$  in the large angle case. What finally limits the proton maximum energy is escape from the shock turbulence region, as the Larmor radius of the accelerated particles increases in size. Despite the more favourable radiative process, electrons are not able to produce gamma-ray synchrotron energies higher than those due to these protons because the competing synchrotron energy loss severely limits the diffusive shock gain (e.g. Gallant et al., 2000) so, the net result is a similar upper photon cutoff. Because the accelerated particle spectra at the shock as here are not necessarily smooth, it might be expected that a detailed experimental study of radiation from this region of a GRB may reveal a related structure. In turn, such a study may reveal new insight into the magnetic field regime of the GRB environment.

The suggestion by Vietri (1995) that the efficient production in GRB of  $10^{20}$  eV protons constitutes a cosmic ray source, at least in previous epochs, is also supported. This argument depends on the similarity of the burst gamma ray energy output and very high energy cosmic ray energy flux (Vietri, 1995; Waxman, 1995).

Finally, we may conclude that first order Fermi acceleration in the sense of

additive energy change over a number of cycles of magnetic discontinuity crossing, appears to be applicable to  $\Gamma \sim 10^3$  flows where, there is no test particle reflection at the discontinuity. However, the large gradients in particle distribution function appearing in the simulations argue against a spatial diffusion approximation description of the phenomenon.

## Acknowledgments

We wish to thank Prof. Drury and the unknown referee for their valuable comments and suggestions regarding this work.

## References

- Achterberg, A., Gallant, Y. A., Kirk, J. G. and Guthmann, A. W., 2001, MNRAS, 328, 393.
- Ballard, K. R. and Heavens, A. F., 1991, MNRAS, 251, 438.
- Baring, M. G, 1999, 26th ICRC Salt Lake City, USA, 4, 5.
- Bednarz, J. and Ostrowski, M., 1996, MNRAS, 283, 447.
- Bednarz, J. and Ostrowski, M., 1998, Phys. Rev. Lett., 80, 3911.
- Bell, A. R., 1987, MNRAS, 225, 615.
- Blackman, E. G., Yi, I. and Field, G. B., 1996, ApJ., 473, L79.
- Brainerd, J. J., 1992, ApJ. Lett. 33, 394.
- Ellison, D. C., Jones, F. C., Reynolds, S. P., 1990, ApJ., 360, 702.
- Fenimore, E. E., Epstein, R. I., Ho, C., 1993, A&AS, 97, 59.
- Gallant, Y. A. and Arons, J., 1994, ApJ., 435, 230.
- Gallant, Y. A. and Achterberg, A., 1999, MNRAS, 305L, 6.
- Gallant, Y. A., Achterberg, A., Kirk, J. G., Guthmann, A.W, 2000, (astro-ph/0001509), Proc. 5th Huntsville Gamma-Ray Burst Symposium.
- Hoshino, M., Arons, J., Gallant, Y. A., Langdon, A. B., 1992, ApJ., 390, 454.
- Jones, F. C. and Ellison, D. C., 1991, Sp. Sc. Rev., 58, 259.
- Kirk, J. G. and Schneider, P., 1987a, ApJ., 315, 425.
- Kirk, J. G. and Schneider, P., 1987b, ApJ., 322, 25.
- Kirk, J. G. and Duffy, P., 1999, astro-ph/9905069.
- Kirk, J. G., Guthmann, A. W., Gallant, Y. A., Achterberg, A., 2000, ApJ., 542, 235.
- Lerche, I. and Schramm, D.N., 1977, ApJ., 216, 881.
- Lieu, R., Quenby, J. J., Drolias, B. and Naidu, K., 1994, ApJ., 421, 211.
- Lieu, R., Axford, W. I. and Quenby, J. J., 1989, A&A, 208, 351.
- Lucek, S. G. and Bell, A. R., 1994, MNRAS, 268, 581.
- Marachi, L., Ghisellini, G., Celotti, A., 1992, ApJ., 397L, 5.
- Meli, A. and Quenby, J. J., 2002b, Ast.Part. Phys. (accepted).
- Meszáros, P. and Rees, M. J. 1993, ApJ., 405, 278.

Meszaros, P. Laguna, P. and Rees, M. J., 1993, ApJ. 415, 181.  
Moussas, X., Quenby, J. J., Theodosiou-Ekaterinidi, Z., Valdes-Galicia, J. F.,  
Drillia, A. G., Roulias, D., Smith, E. J., 1992, Sol. Phys., 140, 161.  
Narayan, R., Paczynski, B., Piran, T., 1992, ApJ., 395L, 83.  
Protheroe, R. J., 2001, 27th ICRC Hamburg, Germany, 6, 2014.  
Protheroe, R. J., Meli, A., and A.-C. Donea, 2002, WISER 2002, Adelaide,  
Sp. Sc. Rev. (accepted).  
Quenby, J. J. and Lieu, R., 1989, Nature, 342, 654.  
Vietri, M., 1998, ApJ. Lett., 448, L105.  
Vietri, M., 1995, ApJ., 453, 883.  
van Putten, M. H. P. M., 2001, Ph. Rep., 345, 1.  
Waxman, E., 1995, Phys. Rev. Lett., 75, 386.